Supporting Information

Surface Evolution of PtCu Alloy Shell over Pd Nanocrystals Leads to Superior Hydrogen Evolution and Oxygen Reduction Reactions

Mingjun Bao[†], Ibrahim Saana Amiinu[†], Tao Peng[‡], Wenqiang Li[†], Shaojun Liu[†], Zhe Wang[†], Zonghua Pu[†], Daping He*[,†,§], Yuli Xiong*[,∥], Shichun Mu*[,†]

[†]State Key Laboratory of Advanced Technology for Materials Synthesis and Processing, Wuhan University of Technology, Wuhan 430070, China

[‡]Department of Civil and Environmental Engineering, University of Windsor, 401 Sunset Ave., Windsor, Ontario N9B 3P4, Canada

[§]Hubei Engineering Research Center of RF-Microwave Technology and Application, Wuhan University of Technology, Wuhan 430070, China

[∥]Michael Grätzel Center for Mesoscopic Solar Cells (MGC), Wuhan National Laboratory for Optoelectronics, School of Optical and Electronic Information, Huazhong University of Science and Technology, Wuhan 430074, China

Correspondence should be addressed to:

* E-mail: hedaping@whut.edu.cn or msc@whut.edu.cn

Experimental Section

Chemicals and Materials: ethylene glycol (EG, AR), isopropyl alcohol (AR), palladium(II) chloride ($PdCl_2$, AR), chloroplatinic acid hexahydrate ($H_2PtCl_6 \cdot 6H_2O$), hydrochloric acid (HCl, 37%), acetic acid (99.7%), perchloric acid ($HClO_4$, 70%), ethanol (AR) and Poly(vinylpyrrolidone) (PVP, Mw~55000) were all purchased from Sinopharm Chemical Reagent CO,.Ltd, China. Cupric acetate anhydrous ($C_4H_6CuO_4$, AR, 98%) was obtained from MACKLIN. Pt/C (20 wt %) and Nafion (5 wt %) were purchased from Sigma-Aldrich. We used all these chemicals as received without any further treatments, and prepared all aqueous solutions were prepared using deionized (DI) water with a resistivity of 18.2 MΩ cm.

Preparation of Pd seeds: In the typical synthesis of Pd seeds, first, 44.3 mg $PdCl_2$ was added into a 10 mL beaker with 87 μL concentrated hydrochloric acid, then sonicated for 20 min until $PdCl_2$ was all dissolved. After that, the solution was mixed with 5 mL ethylene glycol (EG) and sonicated for another 20 min to form Pd precursor solution. In another beaker, 3 g PVP (Mw~55000) was dissolved in 200 ml ethylene glycol (EG) and sonicated until the solution was transparent. Then 2 mL of the transparent solution was pipetted into a flask and preheated at 160 ℃ in oil bath for 20 min. After that, 1 mL of above Pd precursor solution was pipetted into the flask, 35 μL and concentrated hydrochloric acid was also injected into the flask. Finally, the reaction was allowed to proceed for 3 hours.

Synthesis of Pd@Pt core-shell nanocrystals: First, the oil bath temperature was raised to 180 ℃ and preheated for 20 min under vigorous stirring. Then, 2.5 mL $H_2PtCl_6 \cdot 6H_2O$ ethylene glycol solution (4mg/mL) was injected drop by drop into the flask. The reaction was maintained at 180 ℃ for 3 h. Finally, the flask was quenched in an ice-water bath. The products were collected by centrifugation and washed three times with ethanol.

Synthesis of Pd@PtCu core-shell nanocrystals: In another flask, the same amount of Pd seeds were prepared by above method. Then, the oil bath temperature was

raised to 180 ℃ and preheated for 20 min under vigorous stirring. 6.9 mg cupric acetate anhydrous was dissolved in 1.25 mL $H_2PtCl_6 \cdot 6H_2O$ ethylene glycol solution (4mg/mL) and injected drop by drop into the flask. The reaction was maintained at 180 ℃ for 3 h. Finally, the flask was quenched in an ice-water bath. The products were collected by centrifugation and washed three times with ethanol.

Preparation of Pd@Pt NPs/C and Pd@PtCu NPs/C catalysts: The synthesized Pd@Pt or Pd@PtCu NPs and carbon black (Cabot, Vulcan XC-72) were mixed in 10 mL ethanol and sonicated for 3 h to deposit the NPs on the carbon, with the metal loading kept at ~20 % at the same time. Then the products were collected by centrifugation with ethanol for one time. The precipitate was redispersed in 10 mL acetic acid and sonicated for 6 h at 60 ℃ to remove the surface organic matter. At last, the as-prepared Pd@Pt NPs/C and Pd@PtCu NPs/C were washed with ethanol for five times. The final products were dried in vacuum oven at 60 ℃.

Details of theoretical calculations: Density Functional Theory (DFT) computations were performed using the Cambridge Sequential Total Energy Package (CASTEP) based on the plane-wave pseudopotential method. The geometrical structure based on the (111) plane of pure Pd and the (111) plane of PtCu alloy were optimized using the generalized gradient approximation (GGA) method. The electron exchange correlation (EEC) interactions were treated using the Revised Perdew-Burke-Ernzerhof (RPBE) functional. A plane-wave basis set cut-off energy of 400 eV was applied, and a Monkhorst Pack k-point (MPk) grid of 3×3×1 for sampling the Brillouin zone. The cell structures were optimized for force and energy convergence threshold set at 10^{-5} eV and 0.03 eV $Å^{-1}$, respectively. To avoid periodic interactions, a vacuum space as large as 15.0 Å was applied along the direction of the z-axis with a self-consistence field of 2.0×10^{-6} eV/atom. For the valence electrons and ionic core interactions, the ultra-soft pseudopotential was applied. To mimic the sample catalyst properties, the top two surface atomic layers were fully relaxed while the remaining layers were constrained. The free energy (ΔG_{H^*}) for chemisorbed hydrogen was computed as:

$$\Delta G_{H^*} = E_{total} + E_{surf} - \frac{1}{2}E_{H2} + \Delta ZPE - T\Delta S$$

The symbols represent total energy (E_{total}) of the adsorbed system, energy of the pure structure (E_{surf}), change in zero-point-energy (ΔE_{ZPE}), the temperature (T), and change in entropy (ΔS), respectively. Here, the vibrational entropy of H in the adsorbed state is approximately negligible such that $\Delta S_H \approx [S_{H^*} - \frac{1}{2}S_{(H2)}] \approx [-\frac{1}{2}S_{(H2)}]$, where $[-\frac{1}{2}S_{(H2)}]$ denotes the entropy of hydrogen in the gas phase under standard conditions. The standard $[TS_{(H2)}]$ of H_2 is given to be ~0.41 eV at 1 atm and 300 K.[1,2]

The representative models for the catalyst samples were built to simulate Pd (111), PtCu alloy and the Pd@PtCu alloy system. Typically, the (111) facet of PtCu alloy was modeled by the slab with layers of Pt-Cu bonding atoms, and the (111) facet of Pd was adopted to generate the slab for the pure Pd clusters. To create the Pd@PtCu core-shell system, a single layer of Pt-Cu alloy cluster was laid over the Pd surface and optimized. To minimize lattice mismatch, an interface periodicity of 3×2 supercell for Pd phase and 2×2 supercell for the PtCu were applied for creating the simulation model of Pd@PtCu.

Material characterizations: The inductively coupled plasma-optical emission spectra (ICP-OES), Prodigy 7 (LEEMANLABSINC, American) was used to measure the metal contents. Powder X-ray diffraction (XRD) patterns were collected on a D8 Advance (Bruker AXS, Germany) X-ray diffractometer equipped with a Cu Kα radiation source. The morphology and structure were characterized by transmission electron microscopy (TEM, JEM-2100F, JEOL, Japan) and aberration-corrected HRTEM (Titan G2 60-300 with image corrector, American). Energy dispersive spectrometer (EDS) was used to test the composition and elemental distribution of the samples. X-ray photoelectron spectroscopy (XPS) was performed on an ESCALABMK II X-ray photoelectron spectrometer to characterize the chemical composition and valence state of elements the near surface layer.

Electrochemical measurements: A three-electrode cell was used to perform the electrochemical measurements on a CHI660E workstation (Chenhua Instruments, Shanghai, China) at room temperature. The working electrode was a glassy-carbon Rotating Disk Electrode (RDE) (area: 0.196 cm^2 for ORR and, area: 0.0707 cm^2 for HER). A graphite rod was used as the counter electrode, a saturated calomel electrode (SCE) was used as the reference electrode for the acidic electrochemical measurements and a Ag/AgCl electrode as the reference electrode for the alkaline electrochemical measurements, respectively. The catalyst ink was prepared by ultrasonically mixing 3 mg catalysts with 680 μL of isopropyl alcohol, 300 μL of DI water and 20 μL of 5 wt% Nafion solution for 30 min. A certain amount of the catalyst ink was deposited on a glassy carbon electrode to make sure the loading amount of Pt for all the catalysts was 15 $\mu g/cm^2$ for all ORR and HER tests. ORR measurements were conducted in a 0.1 M $HClO_4$ solution bubbled with oxygen during the measurement. The scan and rotation rates for ORR measurement were 5 mV/s and 1600 rpm. The stability of the catalysts were measured by ADT in O_2-saturated 0.1 M $HClO_4$ solutions at room temperature by applying the cyclic potential sweeps from 0.6 to 1.0 V versus RHE at a sweep rate of 100 mV/s for 5000 cycles. For HER measurements, the polarization data were obtained at a scan rate of 5 mV/s in a 0.5 M H_2SO_4 solution for acidic medium HER measurements and a 0.1 M KOH solution for alkaline medium HER measurements. The durability test were measured by ADT at room temperature by applying the cyclic potential sweeps from 0.5 to -1.5 V versus RHE at a sweep rate of 100 mV/s for 10000 cycles. In all measurements, the reference electrode was calibrated with respect to the reversible hydrogen electrode (RHE) and all polarization curves were *iR*-corrected. The calculation equation is $E = U - iR$, E is the potential after correction, U represents the experimentally measured potential, *i* represents the current, and *R* is the solution resistance. For comparison, commercial Pt/C was used as the baseline catalyst with the Pt loading amount of 15 $\mu g/cm^2$ for ORR and HER. All electrochemical experiments were performed at room temperature.

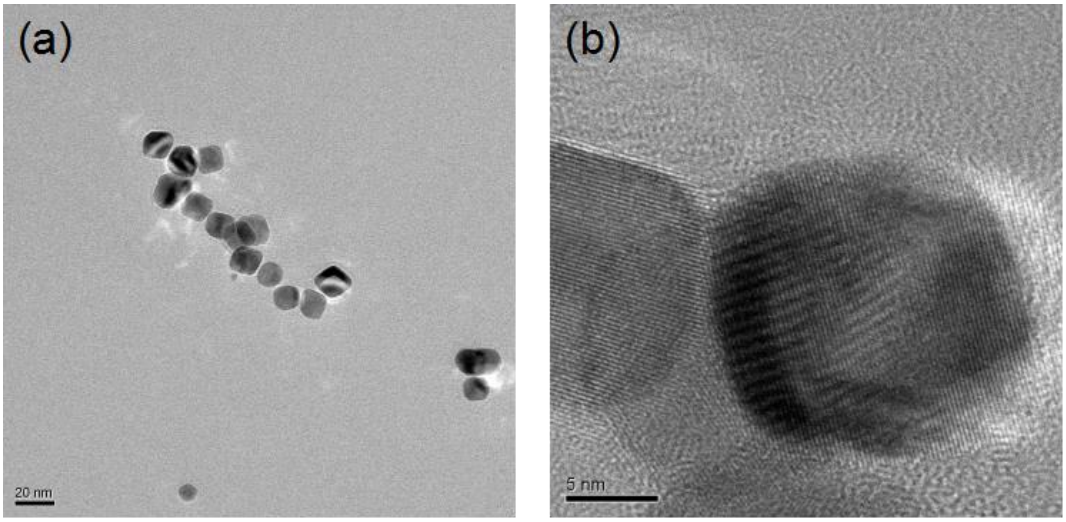

Figure S1. TEM of Pd nanocrystals as seeds: (a) low magnification, (b) high magnification.

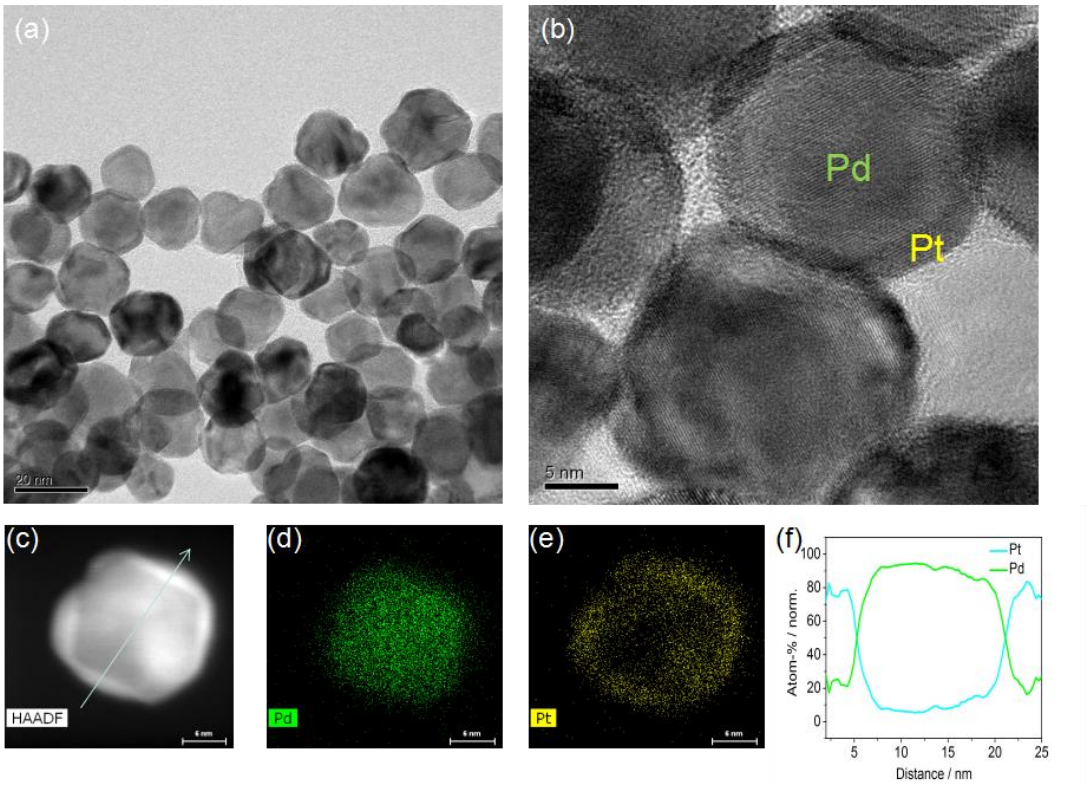

Figure S2. (a) Low and (b) high magnification TEM images of as prepared Pd@Pt core-shell nanoparticles. (c) HAADF-STEM image of Pd@Pt core-shell nanoparticles. (d) Pd and (e) Pt signal of EDX mapping. (f) EDS line scans of Pd and Pt along the arrowed line in (c) recorded from a Pd@Pt core-shell nanoparticle.

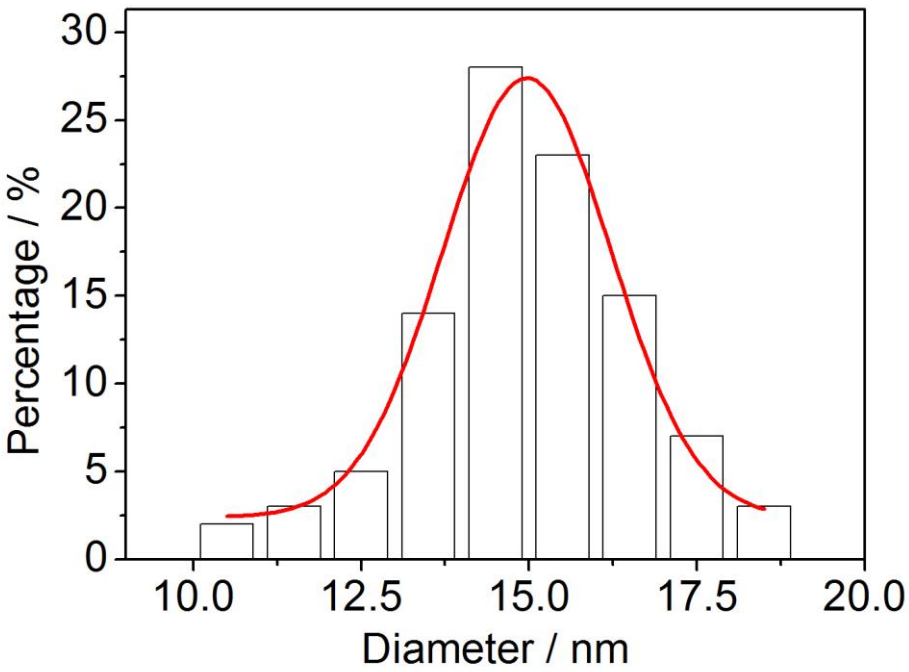

Figure S3. Particle size distribution of Pd@PtCu dodecahedral particles.

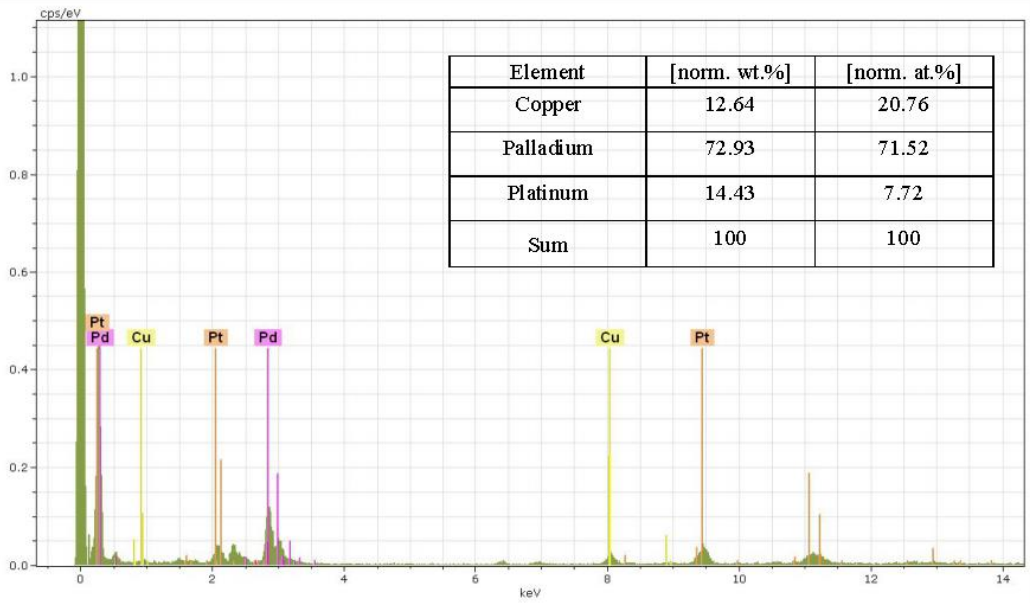

Element	[norm. wt.%]	[norm. at.%]
Copper	12.64	20.76
Palladium	72.93	71.52
Platinum	14.43	7.72
Sum	100	100

Figure S4. EDS of Pd@PtCu core-shell nanoparticles.

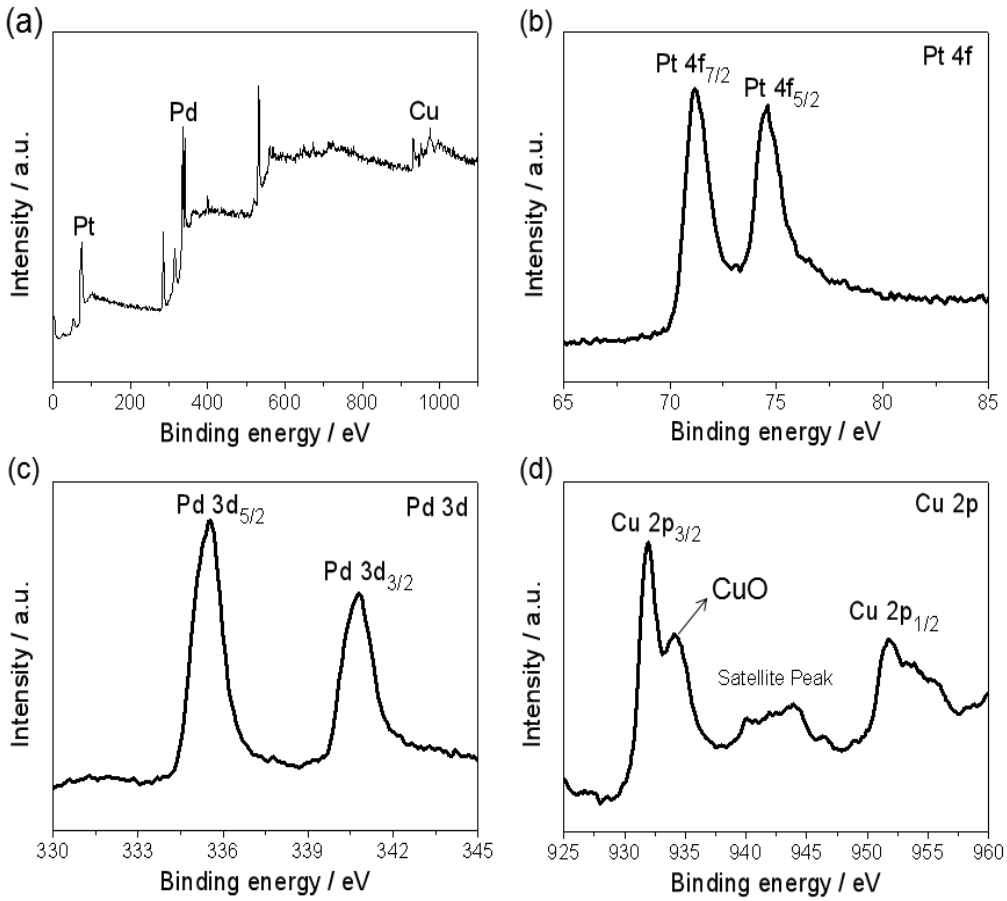

Figure S5. XPS spectra of the Pd@PtCu core-shell nanoparticles: (a) survey, (b) Pt 4f, (c) Pd 3d and (d) Cu 2p.

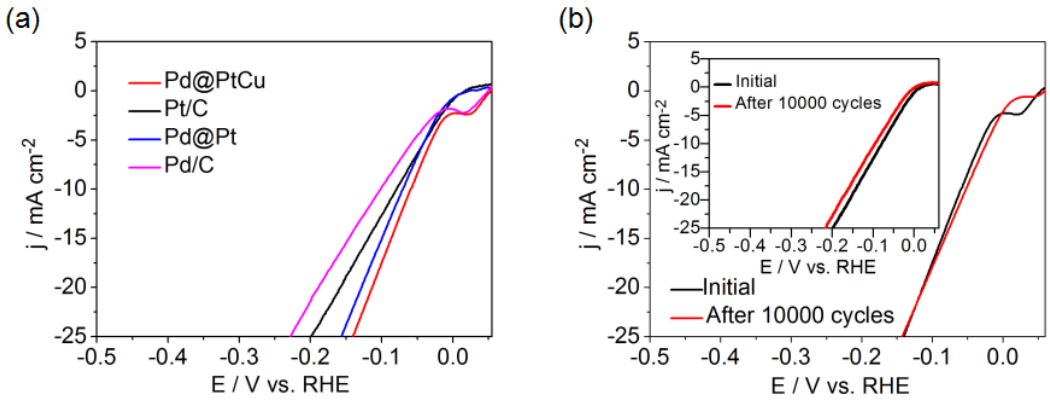

Figure S6. (a) HER polarization curves of Pd@PtCu/C, Pd@Pt/C, Pd/C and Pt/C by LSV with a scan rate of 5 mV/s in 0.1 M KOH at room temperature. (b) Durability of Pd@PtCu/C versus Pt/C catalyst (inset figure). The polarization curves were recorded before and after 10000 CV sweeps between +0.05 and -0.15 V in 0.1 M KOH at room temperature with a scan rate of 5 mV/s.

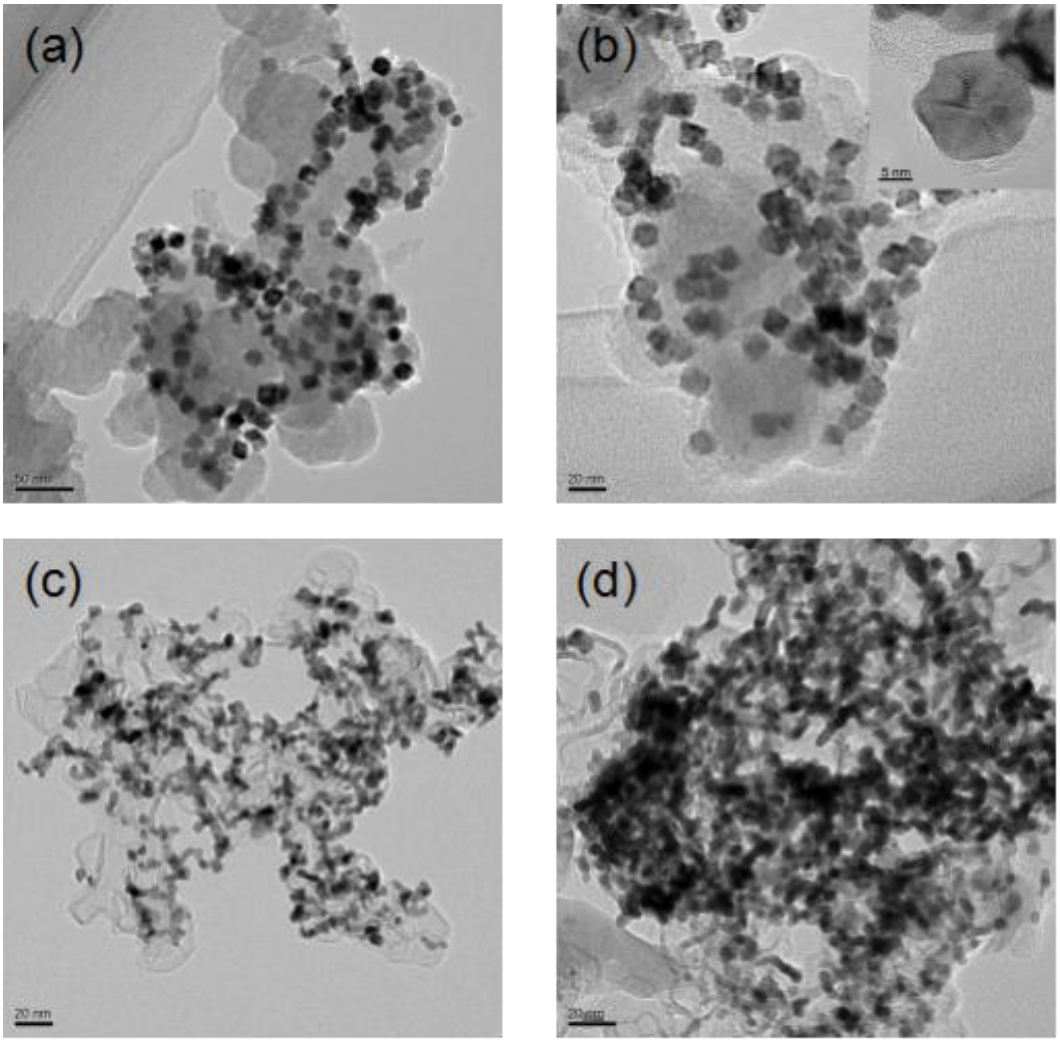

Figure S7. TEM images of Pd@PtCu/C catalyst before (a) and after (b with inset of HETEM image) 5000 cycles by ADT, and Pt/C catalyst before (c) and after (d) 5000 cycles by ADT.

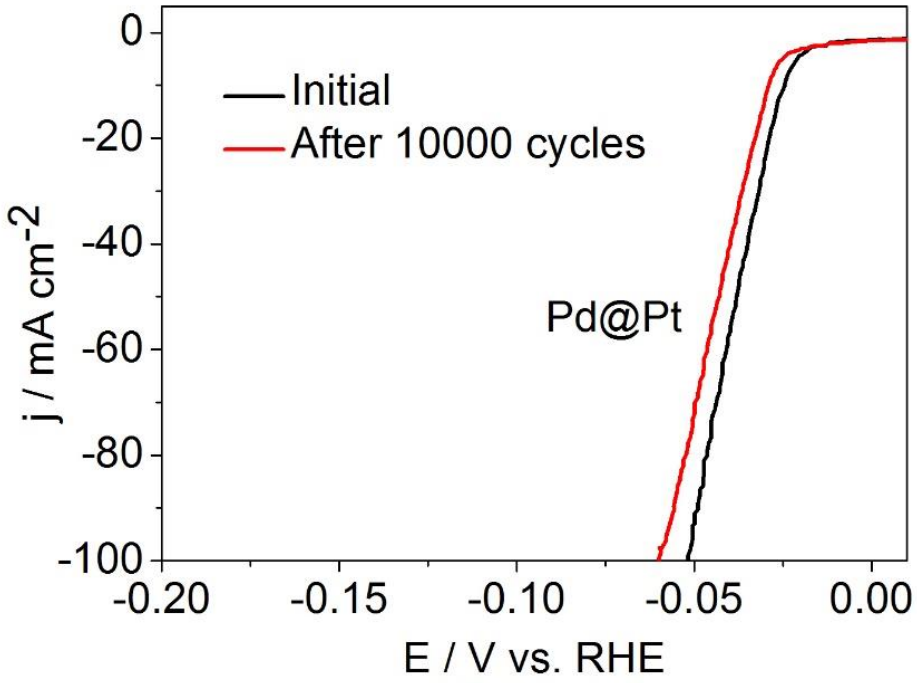

Figure S8. HER durability of Pd@Pt/C. The polarization curves were recorded before and after 10000 CV sweeps between +0.05 and -0.15 V in 0.5 M H_2SO_4 at room temperature with a scan rate of 5 mV/s.

Table S1 Comparison of HER performance in acid and alkaline media for Pd@PtCu/C with other HER electrocatalysts.

Catalysts	**Electrolytes/ (pH)**	**Overpotential@j (mV@mA cm^{-2})**	**Tafel slope (mV dec^{-1})**	**Catalyst loading (mg cm^{-2})**	Ref.
Pd@PtCu/C	0.5 M H_2SO_4	19@10	26.2	0.15	This work
	0.1 M KOH	60@10	-		
Pd/Pt(poly)	0.1 M NaOH	~110@10	53	-	3
Pd-Mn_3O_4	0.5 M KOH	115@10	-	-	4
	0.5 M H_2SO_4	14@10	42		
CoPd@NC	0.5 M H_2SO_4	80@10	31	0.285	5
C_3N_4/Pd	0.5 M H_2SO_4	339@10	116	1.056	6
Ni@Ni(OH)$_2$/Pd/rGO	1 M KOH	76@10	70	0.25	7
Pd–C_3N_4	0.5 M H_2SO_4	55@10	35	0.043	8
N-Doped CNTs supported Pd	0.5 M H_2SO_4	300@60	-	0.7	9
Au-Pd-MWCCE	0.1 M HCl	300@3	136	-	10
Au–Pd/CFP	0.5 M H_2SO_4	~90@10	47	0.5	11
Pd/HOPG	0.5 M H_2SO_4	~150@10	118.3	-	12
Pd cube/PEI-rGO50:1	0.5 M H_2SO_4	108@100	34	0.14	13
PdTe NMs/rGO	1 M KOH	97@10	-	0.28	14
Pt/WC	0.1 M $HClO_4$	~200@10	40	0.3	15
Pt@NHPCP	0.1 M $HClO_4$	57@10	27	0.002	16
ALD50Pt/NGNs	0.5 M H_2SO_4	50@16	29	0.077	17
hcp Pt–Ni	0.1 M KOH	65@10	78	0.061	18
Pt/CFs	0.5 M H_2SO_4	~220@100	53.6	-	19

Pt NWs/SL-Ni(OH)	0.1 M KOH	57.8@4	-	-	20
	1 M KOH	85.5@4	-		
Pt(pc) electrode	0.1 M KOH	70@2.4	-	-	21
	1 M KOH	70@1.7	-		
$Ni(OH)_2$ modified Pt surface	0.1 M KOH	~95@4	-	-	22
Pt_3Ni frames/$Ni(OH)_2$/C	0.1 M KOH	~59@4	-	-	23

References

1. Nørskov, K.; Bligaard, T.; Logadottir, A.; Kitchin, J. R.; Chen, J. G.; Pandelov, S.; Stimming, U. Trends in the exchange current for hydrogen evolution. *J. Electrochem. Soc.* **2005**, *152*, J23-J26.
2. Liu, Y.; Yu, G.; Li, G.-D.; Sun, Y.; Asefa, T.; Chen, W.; Zou. X. Coupling Mo_2C with Nitrogen-Rich Nanocarbon Leads to Efficient Hydrogen-Evolution Electrocatalytic Sites. *Angew. Chem. Int. Ed.* **2015**, *54*, 10752-10757.
3. Smiljanic, M.; Rakocevic, Z.; Maksic, A.; Strbac, S. Hydrogen evolution reaction on platinum catalyzed by palladium and rhodium nanoislands. *Electrochimica Acta* **2014**, *117*, 336-343.
4. Ray, C.; Dutta, S.; Negishi, Y.; Pal, T. A new stable Pd-Mn_3O_4 nanocomposite as an efficient electrocatalyst for the hydrogen evolution reaction. *Chem. Commun*. **2016**, *52*, 6095-6098.
5. Chen, J.; Xia, G.; Jiang, P.; Yang, Y.; Li, R.; Shi, R.; Su, J.; Chen, Q. Active and Durable Hydrogen Evolution Reaction Catalyst Derived from Pd-Doped Metal-Organic Frameworks. *ACS Appl. Mater. Interfaces* **2016**, *8*, 13378-13383.
6. Nazir, R.; Fageria, P.; Basu, M.; Gangopadhyay, S.; Pande, S. Decoration of Pd and Pt nanoparticles on a carbon nitride (C_3N_4) surface for nitro-compounds reduction and hydrogen evolution reaction. *New J. Chem.* **2017**, *41*, 9658-9667.
7. Deng, Z.; Wang, J.; Nie, Y.; Wei, Z. Tuning the interface of Ni@$Ni(OH)_2$/Pd/rGO catalyst to enhance hydrogen evolution activity and stability. *J. Power Sources* **2017**, *352*, 26-33.
8. Bhowmik, T.; Kundu, M. K.; Barman, S. Palladium Nanoparticle-Graphitic Carbon Nitride Porous Synergistic Catalyst for Hydrogen Evolution/Oxidation Reactions over a Broad Range of pH and Correlation of Its Catalytic Activity with Measured Hydrogen Binding Energy. *ACS Catal.* **2016**, *6*, 1929-1941.
9. Ramakrishna, S.U.B.; Reddy, D. S.; Kumar, S. S.; Himabindu, V. Nitrogen doped CNTs supported Palladium electrocatalyst for hydrogen evolution reaction in PEM water electrolyser. *Int. J. Hydrogen Energy* **2016**, *41*, 20447-20454.

10. Abbaspour, A.; Norouz-Sarvestani, F. High electrocatalytic effect of Au-Pd alloy nanoparticles electrodeposited on microwave assisted sol-gel-derived carbon ceramic electrode for hydrogen evolution reaction. *Int. J. Hydrogen Energy* **2013**, *38*, 1883-1891.
11. Zhuang, Z.; Wang, F.; Naidu, R.; Chen, Z. Biosynthesis of Pd-Au alloys on carbon fiber paper: Towards an eco-friendly solution for catalysts fabrication. *J. Power Sources* **2015**, *291*, 132-137.
12. Ju, W.; Brülle, T.; Favaro, M.; Perini, L.; Durante, C.; Schneider, O.; Stimming, U. Palladium Nanoparticles Supported on Highly Oriented Pyrolytic Graphite: Preparation, Reactivity and Stability. *ChemElectroChem* **2015**, *2*, 547-558.
13. Li, J.; Zhou, P.; Li, F.; Ma, J.; Liu, Y.; Zhang, X.; Huo, H.; Jin, J.; Ma, J. Shape-controlled synthesis of Pd polyhedron supported on polyethyleneimine-reduced graphene oxide for enhancing the efficiency of hydrogen evolution reaction. *J. Power Sources* **2016**, *302*, 343-351.
14. Jiao, L.; Li, F.; Li, X.; Ren, R.; Li, J.; Zhou, X.; Jin, J.; Li, R. Ultrathin PdTe Nanowires Anchoring Reduced Graphene Oxide Cathodes for Efficient Hydrogen Evolution Reaction. *Nanoscale* **2015**, *7*, 18441-18445.
15. Liu, Y.; Mustain, W. E. Evaluation of tungsten carbide as the electrocatalyst support for platinum hydrogen evolution/oxidation catalysts. *Int. J. Hydrogen Energy* **2012**, *37*, 8929-8938.
16. Ying, J.; Jiang, G.; Cano, Z. P.; Han, L.; Yang, X. Y.; Chen, Z. Nitrogen-doped hollow porous carbon polyhedrons embedded with highly dispersed Pt nanoparticles as a highly efficient and stable hydrogen evolution electrocatalyst. *Nano Energy* **2017**, *40*, 88-94.
17. Cheng, N.; Stambula, S.; Wang, D.; Banis, M. N.; Liu, J.; Riese, A.; Xiao, B.; Li, R.; Sham, T. K.; Liu, L. M.; *et al*. Platinum single-atom and cluster catalysis of the hydrogen evolution reaction. *Nat. Commun*. 2016, *7*, 13638.
18. Cao, Z.; Chen, Q.; Zhang, J.; Li, H.; Jiang, Y.; Shen, S.; Fu, G.; Lu, B.; Xie, Z.; Zheng, L. Platinum-nickel alloy excavated nano-multipods with hexagonal close-packed structure and superior activity towards hydrogen evolution reaction.

Nat. Commun. 2017, *8*, 15131.

19. Hou, D.; Zhou, W.; Liu, X.; Zhou, K.; Xie, J.; Li, G.; Chen, S. Pt nanoparticles/MoS_2 nanosheets/carbon fibers as efficient catalyst for the hydrogen evolution reaction. *Electrochim. Acta* **2015**, *166*, 26-31.
20. Yin, H.; Zhao, S.; Zhao, K.; Muqsit, A.; Tang, H.; Chang, L.; Zhao, H.; Gao, Y.; Tang, Z. Ultrathin platinum nanowires grown on single-layered nickel hydroxide with high hydrogen evolution activity. *Nat. Commun.* **2015**, *6*, 6430.
21. Rheinlander, P.; Henning, S.; Herranz, J.; Gasteiger, H. A. Comparing Hydrogen Oxidation and Evolution Reaction Kinetics on Polycrystalline Platinum in 0.1 M and 1 M KOH. *ECS Trans.* **2013**, *50*, 2163-2174.
22. Danilovic, N.; Subbaraman, R.; Strmcnik, D.; Chang, K. C.; Paulikas, A. P.; Stamenkovic, V. R.; Markovic, N. M. Enhancing the Alkaline Hydrogen Evolution Reaction Activity through the Bifunctionality of $Ni(OH)_2$/Metal Catalysts. *Angew. Chem.* **2012**, *124*, 12663-12666.
23. Chen, C.; Kang, Y.; Huo, Z.; Zhu, Z.; Huang, W.; Xin, H. L.; Snyder, J. D.; Li, D.; Herron, J. A.; Mavrikakis, M.; *et al*. Highly Crystalline Multimetallic Nanoframes with Three-Dimensional Electrocatalytic Surfaces. *Science* 2014, *343*, 1339-1343.